

Hybrid Cross-Laminated Timber under Bending: Finite Element Analysis Based on Nondestructive Testing

József Garab ^{*}

László Bejó

Tamás Király

Faculty of Wood Science and Creative Industries, Institute of Applied Sciences, University of Sopron

Article info

Received: 3 July 2025

Accepted: 29 September 2025

Published: 13 January 2026

Keywords

hardwood

less-used wood species

hybrid cross-laminated timber

bending test

open-source FEM solver

The growing demand for wood as a raw material, coupled with the impacts of climate change on coniferous forests, necessitates research into less-used wood species and potential hardwood alternatives. By integrating material characterisation with computational analysis, this research aims to bridge the gap between resource availability and structural performance. This study focuses on developing a numerical model to simulate the mechanical behavior of softwood, hardwood, and hybrid cross-laminated timbers (CLT) under bending loads within the linear elastic range. The research methodology involved finite element analysis to simulate four-point bending tests on hybrid CLT panels using the open-source FEM solver Code_Aster. Material properties were determined based on Non-Destructive Test (NDT) measurements and literature data. The developed finite element model successfully simulated CLT's response under four-point bending conditions, demonstrating its potential for virtual prototyping of various less-used wood species in CLT applications. The numerical model showed acceptable agreement with experimental results. The relative error varies between 1.30% to 17.37% in the results based on the NDT measurements. The results derived from literature values show higher variation. This computational approach provides a valuable tool for evaluating alternative wood species in engineered wood products.

DOI: 10.53502/wood-211455

This is an open access article under the CC BY 4.0 license:

<https://creativecommons.org/licenses/by/4.0/deed.en>.

Introduction

The need for wood-based materials is steadily rising alongside the expanding population and urbanization. In addition to traditional timber, various engineered wood products are being developed to meet this demand. Developed in Europe at the end of the last century, cross-laminated timber (CLT) features orthogonal orientations of the timber lamellae, allowing it to function as a two-dimensional load-bearing element. This design provides both lightweight properties and

stiffness in both in-plane and out-of-plane directions (Brandner et al., 2016). The expansion of the volume of the CLT is remarkable; CLT panels can be used in prefabricated walls and floor elements. Therefore, usage of CLT is favoured for constructional purposes since its introduction to the market (Gagnon & Pirvu, 2011). Choosing CLT over concrete or masonry also supports sustainability goals.

The use of CLT products as construction material requires a clear understanding of their mechanical properties, including stiffness and strength under various

^{*} Corresponding author: garab.jozsef@uni-sopron.hu

conditions. Therefore, experimental investigations were widely performed on the CLT products and connections. The response of CLT to in-plane loading has been extensively studied, particularly in relation to its application as a wall material (Akter et al., 2021; Amer et al., 2024; Bogensperger et al., 2010; Turesson & Ekevad, 2016). Several studies have also been conducted on the out-of-plane behavior of CLT, demonstrating its suitability for floor applications (Asselstine et al., 2021; Bahrami et al., 2021; Pang & Jeong, 2019).

Evaluating the performance of wood-based composites is complex due to factors such as material heterogeneity and geometry, often resulting in costly and time-consuming experimental procedures. Therefore, numerical simulations offer a valuable alternative to address these challenges in biocomposite performance testing. Numerical simulations were also extensively performed on CLT in order to investigate the physical properties. In addition to the classical mechanical properties, studies have also examined responses related to rheology, moisture-induced stresses, and seismic performance. Sebera et al. (Sebera et al., 2015) analysed the behavior of CLT panels subjected to torsion and established an effective procedure for quick verification of the numerical model for CLT. This methodology can then be applied in the virtual prototyping of CLT products that deviate from standard configurations. Śliwa-Wieczorek et al. (Śliwa-Wieczorek et al., 2023) investigated the creep behaviour and solved numerically as a problem of linear theory of viscoelasticity. Gereke and Niemz studied the moisture-induced stresses in CLT panels (Gereke & Niemz, 2010). They established that delamination occurs when a material undergoes various stresses that are primarily caused by variations in swelling and shrinkage, leading to drying defects. The improvement of the seismic behavior of CLT panels was investigated by Latour and Rizzano through the introduction of dissipative connectors into the structure (Latour & Rizzano, 2017).

Recent research on finite element analysis of CLT for bending applications has yielded significant insights. Studies have demonstrated the accuracy of finite element models in predicting out of plane bending stiffness and strength of CLT panels, considering factors such as layer arrangement (Albostami et al., 2021; Haftkhani & Hematabadi, 2022; Hematabadi et al., 2020) or lamella properties and finger joint strength (Olsson & Abdeljaber, 2024) or layer arrangement. Hybrid CLT panels are made from different wood species layers. Connecting the hybrid CLT material to our study, the beech-poplar hybrid hardwood CLT was in focus for bending and shear stiffness performance assessment study (Hematabadi et al., 2022). Bending stiffness was investigated on diagonal hybrid CLT made from black locust and eastern white pine (Kurzinski & Crovella,

2024) and on poplar and hybrid maple-poplar CLT (Das et al., 2025).

Because of the increasing demand for wood as a raw material, researchers have strived to investigate the usage of less-used wood species and to investigate the potential of hardwood species that can replace dwindling coniferous wood resources due to climate change (Borovics et al., 2023; Király et al., 2024; Verkerk et al., 2022).

To support this using virtual prototyping, a numerical model was developed for simulating the mechanical behavior of softwood, hardwood, and hybrid CLTs in case of bending in the linear elastic range. The performance of the finite element model was compared to our experimental test results (Altaher Omer Ahmed et al., 2023). The input parameters to the material model were taken from two sources: based on measured NDT parameters connected to the EN strength class parameters, and from literature data. The main goal of this study was to investigate if literature data-based analysis is sufficient to model the behavior of hybrid CLT or if applying NDT measurements is needed for better input parameters to the material model. The modelling of the tests relies on free and open-source software to encourage interoperability, adaptability, and accessibility, and could be a basis for further parametric studies. The open-source solver Code_Aster by EDF was utilized in numerous studies to simulate the mechanical behavior of wood and wood-based products or structures (Humbert et al., 2014; Patlakas et al., 2019; Rescalvo et al., 2020; Riparbelli, Dionisi-Vici, et al., 2023; Riparbelli, Mazzanti, et al., 2023). To widen the application area of the open source numerical solutions, the Coder_Aster solver by EDF was used in this study.

Materials and methods

A finite element (FE) model was developed to investigate the structural response of hybrid CLT beams under a 4-point bending, based on the test series from Altaher et al. (Altaher Omer Ahmed et al., 2023).

The experimental study presented an investigation of the viability of some Hungarian hardwood materials for use in CLT materials. Homogeneous beech (*Fagus sylvatica*), poplar (*Populus spp.*), and spruce (*Picea abies*) panels, as well as their combinations, were created using a polyurethane adhesive in a three-layer build-up.

The CLT composite was modelled in the pre-processing phase as a 3D model with the open source SALOME platform (SALOME, 2024). The mesh consists of 33918 fully integrated linear isoparametric continuum elements (HEXA8). The Coder_Aster solver (v14.6) was used for linear static numerical simulation in our current study. To simulate the

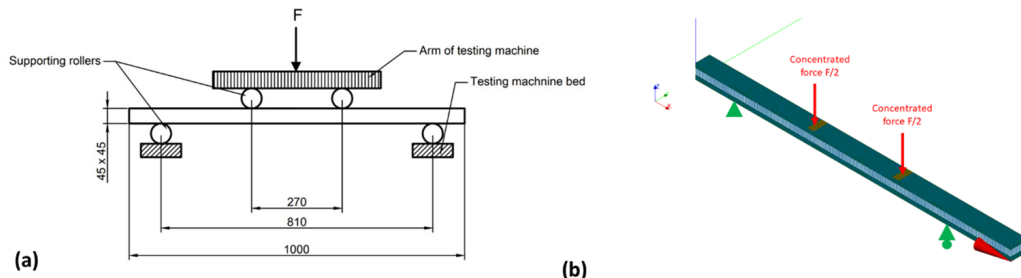


Fig. 1. 4-point bending test according to MSZ EN 408; a – experimental test setup; b – FE model of the test

experimental test, the FE model of the CLT beams considers orthotropic material properties where the longitudinal axis is aligned to the grain direction, the beam width is aligned to the radial direction, and the beam thickness is aligned to the tangential direction. The finite elements in the model have their principal material axes aligned with the orientation of the lamellas in the physical beam (the middle layer is rotated by 90° relative to the top and bottom layers). The orthotropic elastic constants used in the FE model were based on measured material properties and on literature data. Prior to CLT manufacturing, the raw material for the CLTs was graded using the portable lumber grader, PLG + equipment, which was developed at the Jozsef Bodig Wood NDT Laboratory of the University of Sopron (Dívós, 2002). Table 1 demonstrates the specimen combinations for the CLT beams with the strength classes according to MSZ EN 338 (European Standard., 2009). The labels for each group are formed from the first letter of the material type in the top, middle, and bottom layers of the CLT panel (e.g., BPB = Beech-Poplar-Beech). Therefore, the elastic parameters for the top and bottom layers, based on strength grades specified in MSZ EN 338, were applied in the FE model. Figure 1 shows the test layout of the 4 point bending test according to MSZ EN 408 (European Standard., 2010) and the FE model. The applied load was 1500 N, which corresponds to 25% of the ultimate maximum load for the CLT made

from spruce wood. Therefore, the response of the test structure is in the linear elastic range.

Because the full set of orthotropic elastic constants was not measured for the tested materials, the full set of orthotropic elastic constants was derived from MOE (Modulus of Elasticity) parallel to the grain (E_0) and from the shear modulus for planes parallel to the grain (G_0) according to the method applied by Patlakas et al. (Patlakas et al., 2019). The MOE perpendicular to grain E_{90} was considered as a constant fraction of E_0 ($E_0/E_{90}=30$) and the rolling shear modulus G_{90} as a constant fraction of G_0 ($G_0/G_{90}=10$). The three Poisson's ratios were considered equal to 0.35. Table 2 presents orthotropic material properties used in FE simulations according to the strength grades based on NDT measurements.

In addition to the NDT-based simulations, modeling was performed not only based on the NDT-defined strength class parameters, but also based on literature data in order to compare the results in a broader manner. Thus, the orthotropic elastic constants were taken from the literature, which is presented in Table 3 (Hörig, 1933; Keunecke et al., 2008; Milch et al., 2016; Niemz et al., 2015; Sebera et al., 2015; Szalai, 2004). For the traditional material spruce, the older dataset of Hörig (Hörig, 1933) was included to provide a broader basis for comparison and to reflect a wider range of material properties sources. The postprocessing was performed by ParaView 5.13.0.

Table 1. Species combinations used in CLT experiments and in numerical simulations. NDT predicted dominant strength class according to EN 338 is written in parentheses; the values for the middle layers are estimated

Layer type	Orientation	SSS	BBB	PPP	SPS	BPB	BSB
Top Layer	Longitudinal	Spruce (C24)	Beech (D50)	Poplar (C24)	Spruce (C27)	Beech (D50)	Beech (D50)
Middle Layer	Crossband	Spruce (C24)	Beech (D50)	Poplar (C24)	Poplar (C24)	Poplar (C24)	Spruce (C24)
Bottom Layer	Longitudinal	Spruce (C30)	Beech (D50)	Poplar (C27)	Spruce (C30)	Beech (D50)	Beech (D50)

Table 2. Orthotropic material properties used in FE simulations based on NDT measurements

Wood Species	E_L [MPa]	E_R [MPa]	E_T [MPa]	G_{LR} [MPa]	G_{LT} [MPa]	G_{RT} [MPa]	n_{LR} [-]	n_{LT} [-]	n_{RT} [-]
C24	12 000	400	400	750	750	75	0.35	0.35	0.35
C27	11 500	384	384	720	720	72	0.35	0.35	0.35
C30	11 000	367	367	690	690	69	0.35	0.35	0.35
D50	14 000	467	467	930	930	93	0.35	0.35	0.35

Table 3. Orthotropic material properties used in FE simulations from the literature

Wood Species	E_L [MPa]	E_R [MPa]	E_T [MPa]	G_{LR} [MPa]	G_{LT} [MPa]	G_{RT} [MPa]	n_{LR} [-]	n_{LT} [-]	n_{RT} [-]
Norway spruce (Hörig, 1933)	16 200	699	400	628	775	37	0.019	0.013	0.24
Norway Spruce (Szalai, 2004)	13 500	890	480	720	500	32	0.45	0.54	0.56
Norway Spruce (Keunecke et al., 2008)	12 800	625	397	617	587	53	0.018	0.014	0.21
Poplar (Szalai, 2004)	9 700	700	410	720	670	110	0.32	0.39	0.70
Yellow poplar (Sebera et al., 2015)	12 800	1 178	550	960	883	141	0.32	0.39	0.52
Eastern cottonwood (Sebera et al., 2015)	10 340	858	486	786	538	155	0.34	0.42	0.29
European beech (Szalai, 2004)	13 700	2 240	1 140	1 610	1 060	460	0.45	0.51	0.75
European beech (Niemz et al., 2015)	11 060	1 650	750	1240	940	380	0.04	0.04	0.31
European beech (Milch et al., 2016)	13 439	1 880	1 031	1 608	1 059	460	0.073	0.043	0.36

The agreement between numerical simulations and experimental results was evaluated by comparing the mean experimental and simulated load-deflection curves. Deflections were averaged across repetitions on a common load grid (0-1500 N with 1 N step) and interpolated for the simulation. Model accuracy was quantified using the root mean square error (RMSE), the coefficient of determination (R^2), and the relative error at 1500 N load.

Results and discussion

The load-deflection relationships were analysed for all combinations. The numerical results from the NDT-predicted material model were compared to the experimental values (Figure 2). In some cases, minor deviations were observed in the linear relationship between load and deflection. This discrepancy may be attributed to the different grade combinations, alignment of the specimen

in the test fixture, natural variability of the wood, and gluing issues. This phenomenon is visible for the SSS, SPS, BSB, and PPP combinations. However, the slopes of the calculated load-deflection curves aligned well with the linear range of the measured data (after approximately 2 mm deflection).

According to the statistical analysis (Table 4 and Table 5), the numerical model based on NDT predicted material properties showed very good agreement with experiments of BBB, BPB, PPP, and SPS, with high R^2 values (0.97-0.99) and low RMSE (≤ 0.16 mm). Relative errors at 1500 N were minimal for BBB (1.89%) and BPB (1.30%), moderate for SPS (4.20%), and somewhat larger for poplar (11.13%). In contrast, SSS and BSB showed lower predictive accuracy, with higher RMSE (0.44-0.52 mm), reduced R^2 (0.77-0.86), and the largest relative errors (11.28% and 17.37%). The experimental results for SSS and BSB highlight more clearly the deviation from linearity observed

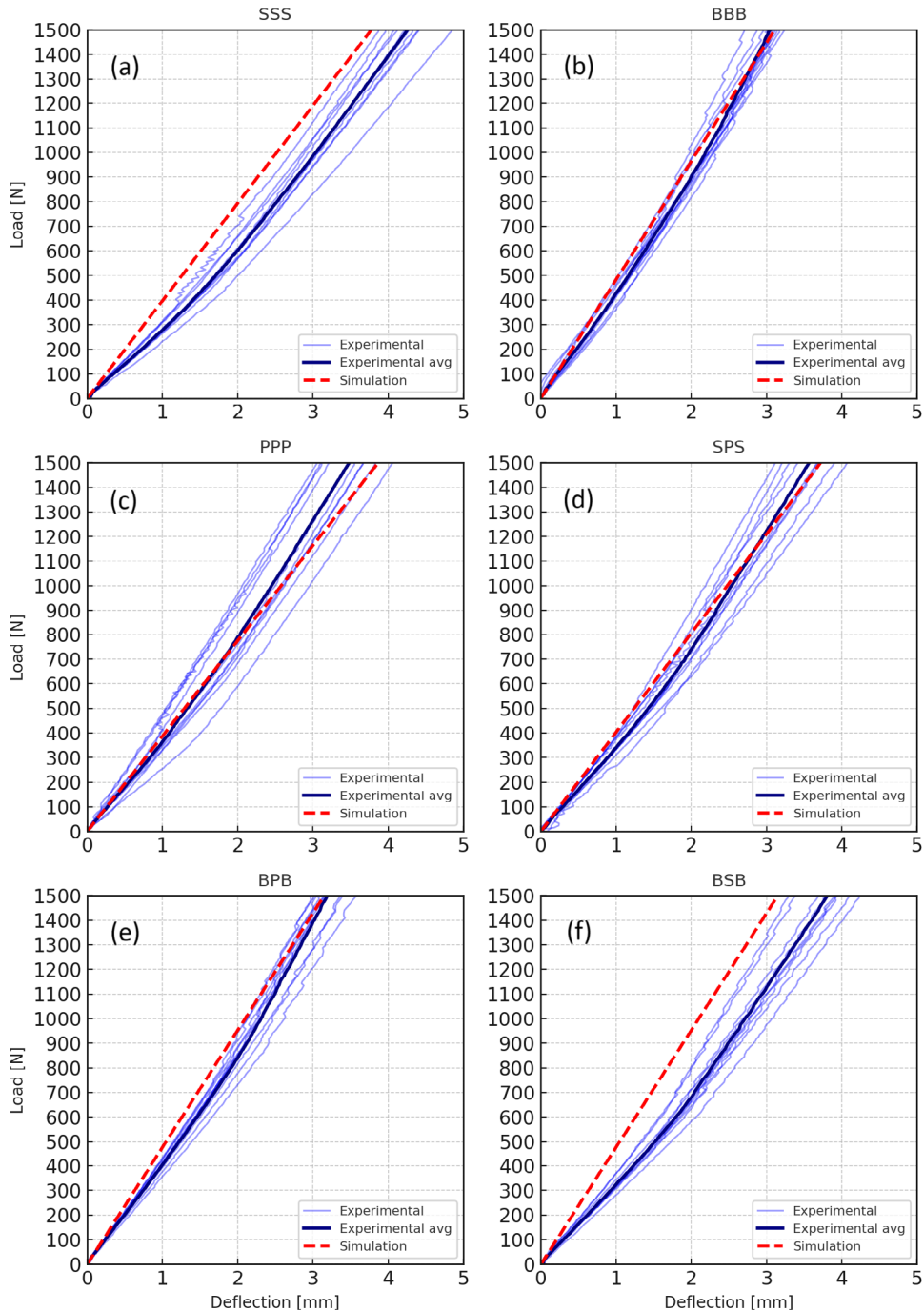


Fig. 2. Experimental and numerical load-deflection curves for the CLT combinations. Individual experimental curves, the experimental average curves, and the simulation curves are presented

at the initial stage of loading. Furthermore, the less favourable performance of the BSB could be attributed to a phenomenon observed during specimen failure, where most BSB specimens failed primarily due to glueline delaminations. The exact reason for this is uncertain, but it is most likely related to the large density difference between the two species. Further discussion of the affected failure mode is detailed with a figure in the experimental part of our research (Altaher Omer Ahmed et al., 2023). It should be noted that the delamination process was not included in the

numerical model at the present stage of the research, which is a significant limitation.

When comparing the numerical results derived from literature-based material properties with the experimental data, the spruce CLT (SSS) datasets showed substantial variation. Simulation results based on the material properties of Keunecke et al. (Keunecke et al., 2008) provided the best agreement with the experiments ($R^2 = 0.73$, $RE=19\%$), while results based on Hörig (1933) deviated most strongly ($R^2 = 0.26$, $RE=36\%$). In contrast, beech (BBB) was

Table 4. Statistical accuracy metrics for experimental and numerical load-deflection curves based on NDT predicted material parameters

Species Combination	Number of experimental curves [pcs]	RMSE [mm]	R ²	Experimental deflection at 1500 N load [mm]	Simulated deflection at 1500 N load [mm]	Relative error at 1500 N load [%]
SSS	10	0.44	0.86	4.26	3.78	11.28
BBB	10	0.10	0.99	3.05	3.11	1.89
PPP	10	0.16	0.97	3.48	3.87	11.13
SPS	10	0.12	0.99	3.57	3.72	4.20
BPB	10	0.16	0.97	3.19	3.15	1.30
BSB	10	0.52	0.77	3.81	3.15	17.37

Table 5. Statistical accuracy metrics for experimental and numerical load-deflection curves based on literature material parameters

Species Combination with material parameter source	Number of experimental curves [pcs]	RMSE [mm]	R ²	Experimental deflection at 1500 N load [mm]	Simulated deflection at 1500 N load [mm]	Relative error at 1500 N load [%]
SSS (Hörig, 1933)	10	1.03	0.26	4.26	2.74	35.69
SSS (Szalai, 2004)	10	0.73	0.62	4.26	3.26	23.49
SSS (Keunecke et al., 2008)	10	0.73	0.62	4.26	3.26	23.49
BBB (Szalai, 2004)	10	0.10	0.99	3.05	3.11	1.89
BBB (Niemz et al., 2015)	10	0.39	0.80	3.05	3.87	26.79
BBB (Milch et al., 2016)	10	0.08	0.99	3.05	3.19	4.51
PPP – Eastern cottonwood (Sebera et al., 2015)	10	0.33	0.89	3.48	4.19	20.32
PPP – Poplar (Szalai, 2004)	10	0.51	0.74	3.48	4.50	29.22
PPP – Yellow poplar (Sebera et al., 2015)	10	0.18	0.97	3.48	3.37	3.23

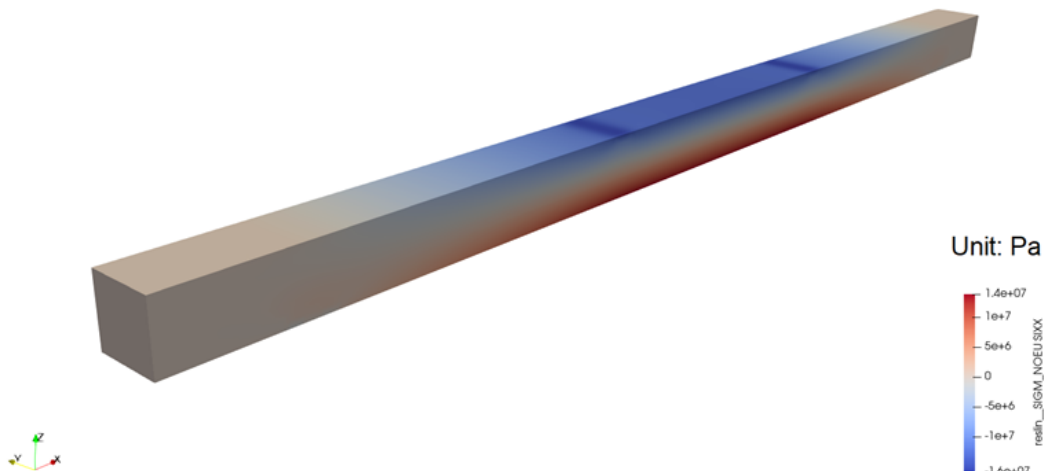
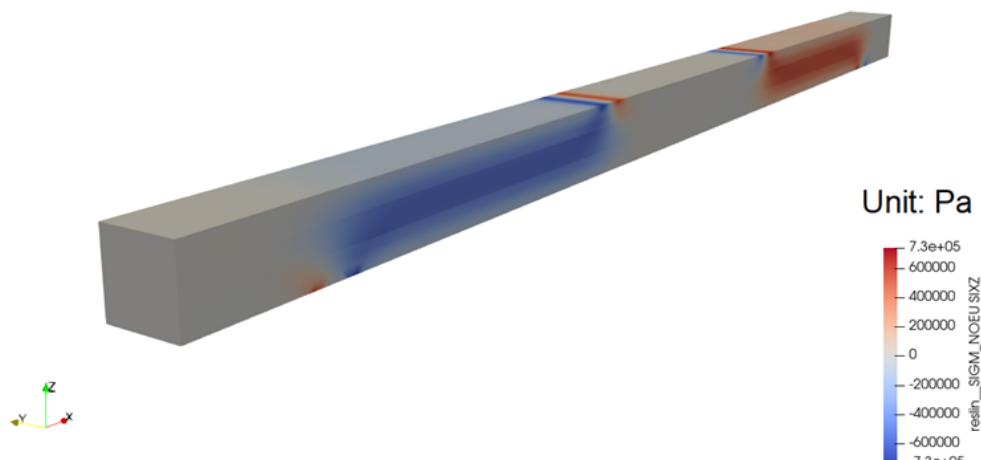
reproduced with excellent accuracy when using the data from Szalai (Szalai, 2004) and Milch et al. (Milch et al., 2016) ($R^2 = 0.99$, $RE \leq 5\%$), whereas results based on Niemz et al. (Niemz et al., 2015) yielded a slightly weaker fit ($R^2 = 0.8$, $RE = 27\%$). For poplar (PPP), the numerical results from the yellow poplar dataset of Sebera et al. (Sebera et al., 2015) gave the closest correspondence to the experimental results ($R^2 = 0.97$, $RE = 3\%$), while Eastern cottonwood and Szalai's poplar values led to a deviation of deflection in the range of 20-29%.

The stresses can be visualized in the specimen according to the simulations. Figure 3 demonstrates the normal stresses in the global X direction, aligned with the longitudinal anatomical main direction of the top and bottom layers of the CLT in the case of the SSS combination. Figure 4 shows the shear stresses in the global XZ plane for the SSS combination.

The stress distributions are the results of a 4-point loading case. The maximum shear stresses are between the applied force and the reaction force at the end of the beam. The maximum normal stresses due to bending are

Table 6. Relative Errors of the numerical and experimental results in the case of bending of CLT-s in the linear elastic range

Study	Focus	Minimum Relative Error [%]	Maximum Relative Error [%]	Note
Navaratnam et al., 2020	Bending and shear performance of Australian Radiata pine cross-laminated timber	Not reported	20	RE for stiffness
Hematabadi et al., 2020	Bending and shear properties of cross-laminated timber panels made of poplar (<i>Populus alba</i>)	3.5	5.2	RE for deflection
Sciomenta et al., 2021	Development and validation of a linear elastic model for three-layered Cross Laminated Timber (CLT) strip slabs	11	22	RE for deflection in
Zhang et al., 2023	Bending and shear performance of a cross-laminated composite consisting of flattened bamboo board and Chinese fir lumber	0.2	6.9	RE for stiffness
Dobes et al., 2023	Stiffness and Deformation Analysis of Cross-Laminated Timber (CLT) Panels Made of Nordic Spruce Based on Experimental Testing, Analytical Calculation, and Numerical Modeling	Not reported	6.4	RE for stiffness

**Fig. 3.** Normal stresses in the global X direction in case of SSS configuration**Fig. 4.** Shear stresses in the global XZ plane in case of SSS configuration

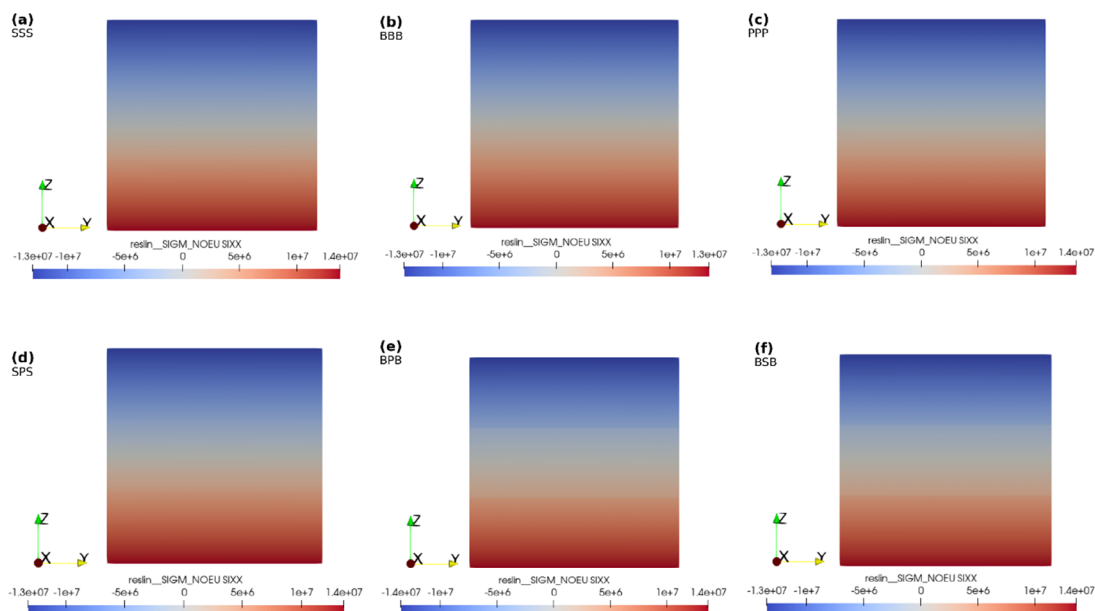


Fig. 5. Normal stresses of the middle sections of the CLT configurations in the global X direction

in the middle of the beam with no shear effect. The bottom part has a tension zone, and the top part has a compression zone. The normal stresses in the axes of the beam direction in the middle sections are visible in Figure 5. The stress field distribution varies slightly in the case of hardwood and softwood hybrid CLTs (Figures 5e and 5f).

Table 6 summarizes the maximum relative errors from the literature between the numerical and experimental results in the linear elastic range. Comparing the relative error from our numerical study to other studies with the literature for displacements in the elastic range, it can be concluded that a maximum 17.37% relative error is within the range of the other studies.

The performed study indicates that numerical results improve when non-destructive testing is incorporated into the procedure. While literature data for material properties can also yield acceptable results, the deviations may be larger. Therefore, the choice of literature sources must be carefully evaluated, considering factors such as the origin of the samples, the methods used to determine the material properties, and the publication date of the source.

Conclusions

The numerical investigations of the 4-point bending test of CLT provided the following key insights:

1. The application of an open-source finite element (FE) solver effectively supports the modeling of cross-laminated timber (CLTs).
2. The linear elastic behavior of the different CLT layups can be adequately modeled if the strength classes of the lamellas are known.

3. NDT-based strength class determination serves as a valuable input for material modeling, especially when literature data is lacking or not complete, as in the case of less-used hardwoods (e.g., Hungarian poplar).
4. The relative errors of the FE results, based on NDT-derived parameters compared to experimental data, range from 1.30% to 17.38%, which is consistent with the range reported in other studies. Therefore, the effectiveness of the applied modeling is confirmed.
5. The FE results based on NDT-derived parameters show better agreement with the experimental results than the FE results based on literature parameters. Given the variability of literature data, elastic constants derived from NDT-based strength classes are preferable for the input to the material model.
6. Consequently, a material model based on NDT-derived parameters serves as a solid starting point for virtual prototyping to investigate mechanical behavior.

Looking ahead, hardwoods will be a primary focus of our future research. Significant efforts will be required to investigate the mechanical properties of less-used or drought-tolerant wood species. Experimentally determined mechanical properties will provide valuable inputs for finite element analysis of timber structures constructed from these species. Therefore, accurately determining the elastic properties and strength of potential hardwood raw materials is a critical priority.

Conflict of interest

The author(s) declare(s) that there is no conflict of interest concerning the publication of this article.

Acknowledgements

This article was produced within the framework of the “TKP2021-NKTA-43” project with the support provided by the Ministry of Innovation and Technology of Hungary from the National Research, Development and Innovation Fund, financed under the TKP2021-NKTA funding scheme.

References

Akter, S. T., Schweigler, M., Serrano, E., & Bader, T. K. (2021). A numerical study of the stiffness and strength of cross-laminated timber wall-to-floor connections under compression perpendicular to the grain. *Buildings*, 11(10). <https://doi.org/10.3390/buildings11100442>

Albostami, A. S., Wu, Z., & Cunningham, L. S. (2021). Elastic response of cross-laminated timber panels using finite element and analytical techniques. *Canadian Journal of Civil Engineering*, 48(10). <https://doi.org/10.1139/cjce-2020-0205>

Altaher Omer Ahmed, A., Garab, J., Horváth-Szováti, E., Kozelka, J., & Bejó, L. (2023). The Bending Properties of Hybrid Cross-Laminated Timber (CLT) Using Various Species Combinations. *Materials*, 16(22). <https://doi.org/10.3390/ma16227153>

Amer, A., Sause, R., & Ricles, J. (2024). Experimental Response and Damage of SC-CLT Shear Walls under Multidirectional Cyclic Lateral Loading. *Journal of Structural Engineering (United States)*, 150(2). <https://doi.org/10.1061/JSENDH.STENG-12576>

Asselstine, J., Lam, F., & Zhang, C. (2021). New edge connection technology for cross laminated timber (CLT) floor slabs promoting two-way action. *Engineering Structures*, 233, 111777. <https://doi.org/10.1016/J.ENGSTRUCT.2020.111777>

Bahrami, A., Vall, A., & Khalaf, A. (2021). Comparison of cross-laminated timber and reinforced concrete floors with regard to load-bearing properties. *Civil Engineering and Architecture*, 9(5). <https://doi.org/10.13189/CEA.2021.090513>

Bogensperger, T., Moosbrugger, T., & Silly, G. (2010). Verification of CLT-plates under loads in plane. *Proceedings of 11th World Conference on Timber Engineering (WCTE2010)*, 885–898.

Borovics, A., Mertl, T., Király, É., & Kottek, P. (2023). Estimation of the Overmature Wood Stock and the Projection of the Maximum Wood Mobilization Potential up to 2100 in Hungary. *Forests*, 14(8). <https://doi.org/10.3390/f14081516>

Brandner, R., Flatscher, G., Ringhofer, A., Schickhofer, G., & Thiel, A. (2016). Cross laminated timber (CLT): overview and development. *European Journal of Wood and Wood Products*, 74(3). <https://doi.org/10.1007/s00107-015-0999-5>

Das, S., Gašparík, M., Sethy, A. K., Niemz, P., Mahapatra, M., Lagaňa, R., Langová, N., & Kytka, T. (2025). Comparative Analysis of Bending and Rolling Shear Performance of Poplar and Hybrid Maple–Poplar Cross-Laminated Timber (CLT). *Journal of Composites Science*, 9(3). <https://doi.org/10.3390/jcs9030134>

Dívós, F. (2002, August 19). Portable lumber grader. *Proceedings of the 13th International Symposium on Nondestructive Testing of Wood*.

Dobeš, P., Lokaj, A., & Vavrušová, K. (2023). Stiffness and Deformation Analysis of Cross-Laminated Timber (CLT) Panels Made of Nordic Spruce Based on Experimental Testing, Analytical Calculation and Numerical Modeling. *Buildings*, 13(1). <https://doi.org/10.3390/buildings13010200>

European Standard. (2009). MSZ EN 338:2009 Structural Timber - Strength classes. European Committee for Standardisation.

European Standard. (2010). MSZ EN 408_2010+A1_2012 Timber Structures - Structural timber and glued laminated timber - Determination of some physical and mechanical properties. European Committee for Standardisation.

Gagnon, S., & Pirvu, C. (2011). Cross laminated timber (CLT) handbook. *FPI Innovations, Vancouver, Canada*.

Gereke, T., & Niemz, P. (2010). Moisture-induced stresses in spruce cross-laminates. *Engineering Structures*, 32(2). <https://doi.org/10.1016/j.engstruct.2009.11.006>

Haftkhani, A. R., & Hematabadi, H. (2022). Effect of Layer Arrangement on Bending Strength of Cross-Laminated Timber (CLT) Manufactured from Poplar (*Populus deltoides* L.). *Buildings*, 12(5). <https://doi.org/10.3390/buildings12050608>

Hematabadi, H., Madhoushi, M., Khazaeyan, A., & Ebrahimi, G. (2022). Performance assessment of bending and shear stiffness of hybrid Beech-Poplar cross-laminated timber (CLT) using experimental and finite element methods. *Iranian Journal of Wood and Paper Science Research*, 37(2), 99–112.

Hematabadi, H., Madhoushi, M., Khazaeyan, A., Ebrahimi, G., Hindman, D., & Loferski, J. (2020). Bending

and shear properties of cross-laminated timber panels made of poplar (*Populus alba*). *Construction and Building Materials*, 265, 120326. <https://doi.org/10.1016/J.CONBUILDMAT.2020.120326>

Hörig, H. (1933). Zur Elastizität des Fichtenholzes. *Zeitschrift Für Technische Physik*, 12, 369–379.

Humbert, J., Boudaud, C., Baroth, J., Hameury, S., & Daudeville, L. (2014). Joints and wood shear walls modelling I: Constitutive law, experimental tests and FE model under quasi-static loading. *Engineering Structures*, 65. <https://doi.org/10.1016/j.engstruct.2014.01.047>

Keunecke, D., Hering, S., & Niemz, P. (2008). Three-dimensional elastic behaviour of common yew and Norway spruce. *Wood Science and Technology*, 42(8). <https://doi.org/10.1007/s00226-008-0192-7>

Király, É., Forsell, N., Schulte, M., Kis-Kovács, G., Börcsök, Z., Kocsis, Z., Kottek, P., Mertl, T., Németh, G., Polgár, A., & others. (2024). Climate change mitigation potentials of wood industry related measures in Hungary. *Mitigation and Adaptation Strategies for Global Change*, 29(6), 62.

Kurzinski, S., & Crovella, P. L. (2024). Investigating the Out-of-Plane Bending Stiffness Properties in Hybrid Species Diagonal-Cross-Laminated Timber Panels. *Applied Sciences*, 14(7). <https://doi.org/10.3390/app14072718>

Latour, M., & Rizzano, G. (2017). Seismic behavior of cross-laminated timber panel buildings equipped with traditional and innovative connectors. *Archives of Civil and Mechanical Engineering*, 17(2), 382–399. <https://doi.org/10.1016/j.acme.2016.11.008>

Milch, J., Tippner, J., Sebera, V., & Brabec, M. (2016). Determination of the elasto-plastic material characteristics of Norway spruce and European beech wood by experimental and numerical analyses. *Holzforschung*, 70(11). <https://doi.org/10.1515/hf-2015-0267>

Navaratnam, S., Christopher, P. B., Ngo, T., & Le, T. V. (2020). Bending and shear performance of Australian Radiata pine cross-laminated timber. *Construction and Building Materials*, 232, 117215. <https://doi.org/10.1016/J.CONBUILDMAT.2019.117215>

Niemz, P., Ozyhar, T., Hering, S., & Sonderegger, W. (2015). Zur orthotropie der physikalisch-mechanischen eenschaften von rotbuchenholz. *Bautechnik*, 92(1). <https://doi.org/10.1002/bate.201400079>

Olsson, A., & Abdeljaber, O. (2024). Predicting out-of-plane bending strength of cross laminated timber: Finite element simulation and experimental validation of homogeneous and inhomogeneous CLT. *Engineering Structures*, 308, 118032. <https://doi.org/10.1016/J.ENGSSTRUCT.2024.118032>

Pang, S. J., & Jeong, G. Y. (2019). Effects of combinations of lamina grade and thickness, and span-to-depth ratios on bending properties of cross-laminated timber (CLT) floor. *Construction and Building Materials*, 222, 142–151. <https://doi.org/10.1016/J.CONBUILDMAT.2019.06.012>

Patlakas, P., Brunetti, M., Christovasilis, I., Nocetti, M., & Pizzo, B. (2019). Structural performance of a novel Interlocking Glued Solid Timber system. *Materials and Structures/Materiaux et Constructions*, 52(1). <https://doi.org/10.1617/s11527-019-1324-2>

Rescalvo, F. J., Rodríguez, M., Bravo, R., Abarkane, C., & Gallego, A. (2020). Acoustic emission and numerical analysis of pine beams retrofitted with FRP and poplar wood. *Materials*, 13(2). <https://doi.org/10.3390/ma13020435>

Riparbelli, L., Dionisi-Vici, P., Mazzanti, P., Brémand, F., Dupré, J. C., Fioravanti, M., Goli, G., Helfer, T., Hesser, F., Jullien, D., Mandron, P., Ravaud, E., Togni, M., Uzielli, L., Badel, E., & Gril, J. (2023). Coupling numerical and experimental methods to characterise the mechanical behaviour of the Mona Lisa: a method to enhance the conservation of panel paintings. *Journal of Cultural Heritage*, 62. <https://doi.org/10.1016/j.culher.2023.06.013>

Riparbelli, L., Mazzanti, P., Manfrani, C., Uzielli, L., Castelli, C., Gualdani, G., Ricciardi, L., Santacesaria, A., Rossi, S., & Fioravanti, M. (2023). Hygromechanical behaviour of wooden panel paintings: classification of their deformation tendencies based on numerical modelling and experimental results. *Heritage Science*, 11(1). <https://doi.org/10.1186/s40494-022-00843-x>

SALOME (9.13.0). (2024). Open CASCADE Technology.

Sciomenta, M., Egidio, A. Di, Bedon, C., & Fragiocomo, M. (2021). Linear model to describe the working of a three layers CLT strip slab: Experimental and numerical validation. *Advances in Structural Engineering*, 24(14). <https://doi.org/10.1177/13694332211020403>

Sebera, V., Muszyński, L., Tippner, J., Noyel, M., Pisaneschi, T., & Sundberg, B. (2015). FE analysis of CLT panel subjected to torsion and verified by DIC. *Materials and Structures/Materiaux et Constructions*, 48(1–2). <https://doi.org/10.1617/s11527-013-0195-1>

Sliwa-Wieczorek, K., Szeptyński, P., Kozik, T., & Gubert, M. (2023). Creep Behavior of CLT Beams with Finite Thickness Layers of Flexible Adhesives. *Materials*, 16(12). <https://doi.org/10.3390/ma16124484>

Szalai, J. (2004). *A faanyag és faalapú anyagok anizotrop rugalmasság- és szilárdság-tána* (2nd ed.). Hillebrand Nyomda.

Turesson, J., & Ekevad, M. (2016). Impact of laminate directions on inplane shear stiffness of crosslaminated timber. *12th Annual Meeting of the Northern European Network for Wood Science and Engineering WSE*, 12–13 September, 2016, Riga, Latvia.

Verkerk, H., Delacote, P., Hurmekoski, E., Kunttu, J., Matthews, R., Mäkipää, R., Mosley, F., Perugini, L., Reyer, C., Roe, S., & others. (2022). *Forest-based climate change mitigation and adaptation in Europe*.

Zhang, X., Yang, S., Fei, B., Qin, D., Yang, J., Li, H., & Wang, X. (2023). Bending and shear performance of a cross-laminated composite consisting of flattened bamboo board and Chinese fir lumber. *Construction and Building Materials*, 392, 131913. <https://doi.org/10.1016/J.CONBUILDMAT.2023.131913>